

Simplified Method for Evaluating Seismic Stability of Steep Slopes

Scott A. Ashford¹ and Nicholas Sitar, M.ASCE²

Abstract: Steep slopes composed of weakly cemented granular soils are common along the Pacific Coast of North America. These slopes, standing at angles of 30° to near vertical, are observed to be prone to seismically induced failures. The steep topography of these slopes makes them particularly susceptible to amplification of seismic waves, and the brittle nature of these materials make deformation-based stability analyses inappropriate. In this paper, a simplified method is presented for assessing the seismic stability of these slopes, utilizing average seismic coefficients to account for the effect of topography. This procedure is based on a review of field and laboratory observations, as well as analyses carried out using generalized consistent transmitting boundaries. The results of the analyses indicate that the amplification due to the soil column in the free field behind the crest dominates the response. The amplification due to topography, on the other hand, shows little variability, and is on the order of 50%. The proposed procedure presented herein gives practicing engineers a method to conduct stability analyses that better represents the actual field conditions for these steep, brittle slopes.

DOI: 10.1061/(ASCE)1090-0241(2002)128:2(119)

CE Database keywords: Seismic stability; Slopes; Granular materials; Stability analysis.

Introduction

The Pacific coastline of the United States and Canada from Southern California to British Columbia is characterized by extensive stretches of steep coastal bluffs in marine terrace deposits, ranging from 20 to 200 m in height. The appearance of the bluffs along this entire stretch of the coast shows evidence of active erosion, and there is abundant historical evidence of slope failures caused by earthquakes, wave erosion, and intense rainfall.

In Northern California, along the stretch of coast from Monterey to San Francisco, seismically induced slope failures occurred during earthquakes in 1865 (Plant and Griggs 1990), in 1906 (Lawson 1908), in 1957 (Bonilla 1959) and, most recently, during the 1989 Loma Prieta (Plant and Griggs 1990; Sitar 1990). The damage caused by these failures was confined to the coastal railroad in 1906 and to the coastal highway in 1957, and there was no direct damage to dwellings because the bluff crests were still largely undeveloped. Since then, the bluff crests along the coast have been extensively developed, particularly in Daly City, Pacifica, Half Moon Bay, Santa Cruz, Capitola, and Seaside (Fig. 1). The 1989 Loma Prieta earthquake demonstrated the risk posed by seismically induced slope failures to these new developments, as shown in Fig. 2. Numerous shallow slides from Pacifica to Rio

Del Mar were responsible for minor damage to structures. Moreover, associated tensile cracking at the crests of the slopes and in some cases loss of crest left many structures more vulnerable to future events. Fortunately, the extent of damage was surprisingly minor considering the severity of other damage in the epicentral region and in San Francisco. Given the apparent potential for damaging landslides during earthquakes, there is a need to develop an improved understanding of the bluff response under seismic loading, and to develop guidelines for stability evaluation of these slopes.

Behavior of Weakly Cemented Sands

The static behavior of weakly cemented soils, which are typical of marine terrace deposits, has been the subject of numerous studies in the recent past (e.g., Haruyama 1973; Clough et al. 1981; Wang 1986; O'Rourke and Crespo 1988; Airey 1993; Das et al. 1995; Puppala et al. 1995; Huang and Airey 1998). Some of the earliest research devoted to cemented sands was performed by Saxena and Lastrico (1978), who studied the static stress-strain behavior of lightly naturally cemented sand with calcite as the cementing agent. They found that the cohesion caused by cementation was the predominant strength component at low strain levels (less than one percent), but the frictional component dominated at high strain levels.

Clough et al. (1981) reported on the results of over 100 tests on naturally and artificially cemented sand. They noted that cemented sand tends to behave in a brittle fashion, with brittleness increasing with cement content and decreasing with increasing confining pressure. Huang and Airey (1998) also concluded that cementation dominated the behavior at low confining pressures. Clough et al. (1981) further found the material to exhibit nearly linear behavior until failure at low confining stresses. Typical tensile strength, determined using the Brazilian tensile test, was determined to be on the order of 10% of the unconfined compressive strength, which was also confirmed by Das et al. (1995). Thus,

¹Assistant Professor, Dept. of Structural Engineering, Univ. of California, San Diego, 9500 Gilman Drive, La Jolla, CA 902093-0085. E-mail: sashford@ucsd.edu

²Professor, Dept. of Civil and Environmental Engineering, Univ. of California at Berkeley, Berkeley, CA 94720. E-mail: nsitar@ce.berkeley.edu

Note. Discussion open until July 1, 2002. Separate discussions must be submitted for individual papers. To extend the closing date by one month, a written request must be filed with the ASCE Managing Editor. The manuscript for this paper was submitted for review and possible publication on December 6, 2000; approved on July 18, 2001. This paper is part of the *Journal of Geotechnical and Geoenvironmental Engineering*, Vol. 128, No. 2, February 1, 2002. ©ASCE, ISSN 1090-0241/2002/2-119-128/\$8.00+\$0.50 per page.

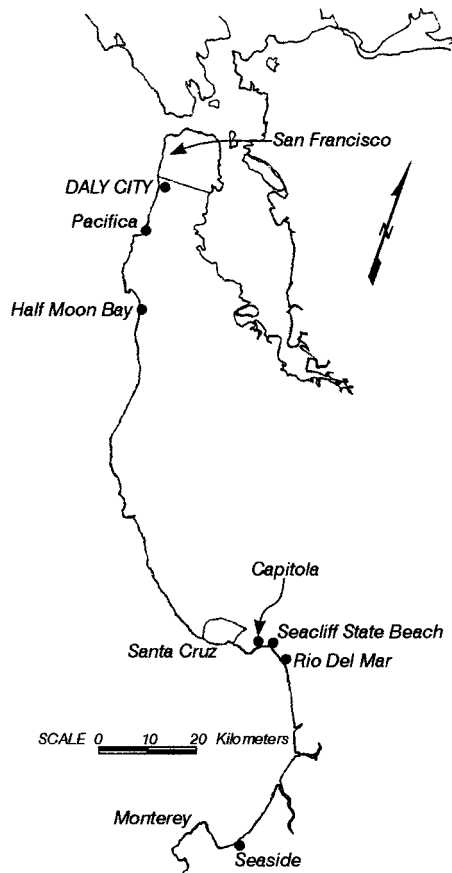


Fig. 1. Location map of coastal developments affected by bluff failures in 1989 Loma Prieta earthquake

the failure envelope curves in the tensile region and gives a lower tensile strength than would be estimated using a straight-line extrapolation of the compression test results.

Fewer studies addressing the dynamic properties of cemented sands are available (e.g., Sitar and Clough 1983; Acar and El-Tahir 1986; Wang 1986; Sitar 1990; Baig et al. 1997). Wang 1986 showed that the stress-strain curve from static tests tend to provide an envelope for the hysteresis loops from cyclic tests. Sitar (1990) suggested that the large strain cyclic stress-strain behavior could be estimated from the results of static testing and showed that there is a trend for reduction in dynamic strength with increasing number of cycles. The effect is most pronounced at low confining pressures where the reduction can be as much as 15%.

The brittle behavior of weakly cemented materials makes for spectacular and potentially devastating slope failures during earthquake loading. In addition to the failures observed along the central coast, many failures have occurred in marine terrace deposits elsewhere in California. The most recent failures include those at Centerville Beach during 1992 Petrolia earthquakes and those at Pacific Palisades (Fig. 3) during the 1994 Northridge earthquake (Ashford and Sitar 1994). In general, very steep slopes (slope angles greater than 60°) in marine terrace deposits fail by toppling or in tension behind the crest followed by shear failure at the base of the block, while moderately steep slopes (those with slope angles between 30° and 60°) tend to fail in shear along a surface subparallel to the slope face (Fig. 4). These modes of failure were previously noted by Sitar and Clough (1983) in their study of seismic slope stability of cemented sands and by O'Rourke and Crespo (1988) based on their study of volcanic soils in Ecuador.

A common characteristic of these failures is that the failure mass at the base of a slide shows an almost complete loss of cementation. There is little evidence of incremental permanent deformations eventually leading up to failure, as is the case with more ductile embankments. Consequently, a failure-based stability analysis, rather than a deformation-based analysis, appears to be more appropriate for these slopes.



Fig. 2. Failure of bluffs in Daly City caused by 1989 Loma Prieta earthquake



Fig. 3. House destroyed in bluff failure at Pacific Palisades during the 1994 Northridge earthquake

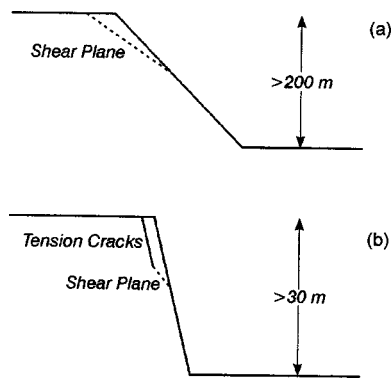


Fig. 4. Typical failure mode for (a) moderately steep and (b) very steep slopes in weakly cemented sands (after Sitar 1990)

Seismic Response Analysis Method

Though there are some studies that specifically consider the seismic response of banks or bluffs (Idriss and Seed 1967; Kovacs et al. 1971; Sitar and Clough 1983), many more studies are available if the seismic response of embankments is considered, and the procedures and concepts developed for embankments may often be extended to banks or bluffs. Newmark (1963) proposed the concept that the stability of an earth dam should be assessed in terms of earthquake-induced deformations, rather than a minimum factor of safety. Newmark (1965) then presented a procedure in which deformations were modeled using the analogy of a sliding block on an inclined plane. Many other researchers used this sliding block analogy in estimating the response of embankments to seismic loading (e.g., Seed and Goodman 1964; Sarma 1975), and more recently Kramer and Smith (1997) for complaint slopes.

Seed and Martin (1966) applied the one-dimensional shear slice method, first proposed by Mononobe et al. (1936), to calculate average seismic coefficients for use in the stability analyses of earth dams. This method simulates the dam as a series of thin horizontal slices. Seed and Martin assumed that (1) that dam is infinitely long and rests on a rigid foundation, (2) the dam is composed of a homogeneous, viscoelastic material, (3) the width to height ratio is large enough so that bending can be neglected

and deformations are only due to shear, (4) the shear stress on any horizontal plane is uniform, and (5) the effect of stored water is negligible. Using this procedure to calculate acceleration time histories throughout the height of the dam, they were able to develop equivalent seismic force series that, in effect, represented the forces acting on the dam during the earthquake. Based on this analysis, an average seismic coefficient was developed that represented the effect of the earthquake on the dam. More recently, Leshchinsky and San (1994) presented average seismic coefficients up to 0.25 g in design charts for assessing the seismic slope stability. Additional background on the use of the seismic coefficients for slope stability analyses can be found in Hynes and Franklin (1984) and Special Publication 117 (Division of Mines and Geology 1997).

Makdisi and Seed (1978), making use of these earlier advances, developed a simple procedure to estimate embankment deformations during earthquakes. This procedure has become a standard of practice for calculating seismically induced embankment deformations. The procedure is based on Newmark's deformation concept and utilizes the average seismic coefficient, as proposed by Seed and Martin (1966), and a yield acceleration that can be calculated by any number of methods. One of Makdisi and Seed's main assumptions is that the embankment material behaves elastically up to yield, but then exhibits perfectly plastic behavior above yield.

The simple and rational approach taken by Makdisi and Seed (1978) is very attractive; however, there are several assumptions in the procedure that do not apply to steep slopes in weakly cemented sand. Most importantly, the brittle nature of weakly cemented sand does not lend itself to a deformation-based analysis, and a factor-of-safety or failure-based analysis is more appropriate.

The intent of our research is to develop a procedure for the analysis of the seismic response and stability of steep natural slopes. This procedure has to account for the semi-infinite extent of the soil mass behind the crest, which is characteristic of many natural slopes. It also has to account for a steep, relatively shallow, planar failure surface. In this context, a simple procedure that allows the estimation of the crest acceleration based on a simple one-dimensional analysis is needed, since the simplified methods used for the analysis of dams (e.g., Makdisi and Seed 1977) are not appropriate for semi-infinite geometries where the shear stress along any given horizontal plane is not uniform.

Computational Model

The computational model used in the study is the generalized consistent transmitting boundary (GCTB) developed and validated by Deng (1991) for two-dimensional seismic site response analysis. The GCTB is an extension of the consistent transmitting boundary, developed by Lysmer and Waas (1972), that allows for a boundary of arbitrary shape. One of the key advances by Deng is the formulation of the solution to the equation of motion along an arbitrarily shaped boundary in a layered system, specifically along a rectilinear curve, and this representation is the basis for the formulation of the GCTB. The prefix "generalized" refers to the ability of these elements to conform to arbitrarily shaped boundaries. The GCTB is formulated by using the exact analytical solution in the horizontal direction and a discretized first- or second-order displacement shape function along the arbitrarily shaped boundary. The frequency-domain model is linear viscoelastic and utilizes the complex response method. An example of a GCTB model for steep slopes is shown in Fig. 5. Additional details on the development and validation of the GCTB can be

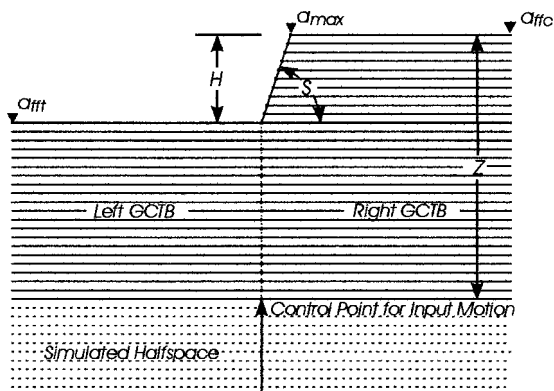


Fig. 5. Example of slope model using pair of generalized consistent transmitting boundaries

found in Deng (1991) and Ashford et al. (1997). Ashford and Sitar (1997) also validated the model for various angles of incidence for shear waves traveling at various directions relative to the face of the slope.

Calculation of k_{av} for Steep Slopes

In defining the average seismic coefficient, k_{av} , Seed and Martin (1966) were able to avoid a summation procedure by assuming that the shear force at the horizontal base of the failure wedge represented the total inertia force induced by the earthquake. In the case of steep slopes, however, the base of the failure surface is steeply inclined (Fig. 4).

If the unit weight is assumed to be constant within the failure wedge, and the absolute acceleration of an individual slice is given in terms of the acceleration of gravity, then the average seismic coefficient can be calculated as

$$k_{av} = \sum \frac{m(y)}{M} \ddot{u}_a(y) \quad (1)$$

where $m(y)$ = mass of the slice at depth y ; M = total mass of the wedge; and $\ddot{u}_a(y)$ = absolute acceleration of slice. This is essentially a "weighted" average.

For the wedge shown in Fig. 6, weight must be given for each slice in order to develop the "weighted" average seismic coefficient from the summation in Eq. (1). The weighting of an individual slice is independent of the slope angle and the angle of the failure surface. Consider the geometry of the potential sliding wedges shown in Fig. 6. Assuming a unit width, it can be easily shown that the weighting, ΔM , given to a horizontal slice (e.g., the slice formed by points DEGF) is given by

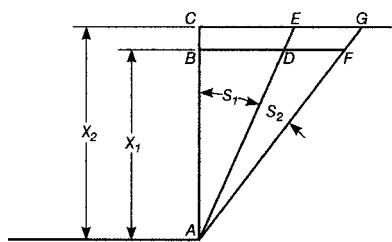


Fig. 6. Wedge-shaped failure surface used to calculate average seismic coefficient for steep slopes

$$\Delta M = \frac{x_2^2 - x_1^2}{x_2^2} \quad (2)$$

From Eq. (2), it can be seen that the weighting factor, ΔM , is independent of the slope angle, S_1 , and the angle of the failure plane, S_2 . This simple result based on the similarity of the triangles simplifies the calculation of the average seismic coefficient for varying slope geometries, if an acceleration value can be determined for each slice.

It is convenient to compute the acceleration that occurs at face of the slope for each slice, rather than obtaining the average value along the slice. While not appropriate for deep-seated failure surfaces in embankment dams, this is a reasonable, though somewhat conservative assumption for the analysis of steep slopes, resulting in overestimation of accelerations by less than 10% (Ashford and Sitar 1994).

In summary, an approach similar to that used by Seed and Martin (1966) and Makdisi and Seed (1977; 1978) can be used to develop average seismic coefficients for steep slopes, as long as the conditions particular to steep slopes are met. In this article, the average seismic coefficient is calculated using a weighted average summation procedure within the potential failure wedge, rather than using the shear slice method, because of the steepness of the failure surface and the semi-infinite extent of the material behind the crest. For convenience, the accelerations used in the analysis herein are those computed at the slope face, which were shown to be reasonable and conservative. Finally, the peak crest acceleration is computed by two-dimensional seismic site response analysis using GCTB.

Site Specific Analyses

Site specific analyses were performed to determine the effect of topography on the seismic response of actual slopes composed of weakly cemented sand. The slopes analyzed include typical sections from three coastal sites in California with a history of seismically induced slope failures: Seacliff State Beach, Daly City, and Pacific Palisades. Field explorations were carried out at the Seacliff and Daly City sites to characterize the subsurface stratigraphy and dynamic soil properties at the sites. The dynamic soil properties of the Pacific Palisades site were assumed to be similar to those of the other two in order to investigate a slope of intermediate height and steepness.

Site Characterization

Site-specific field explorations, including borehole logging and downhole shear wave velocity testing, were carried out at the Seacliff and Daly City sites to characterize the subsurface stratigraphy and dynamic soil properties at the sites. All three sites are underlain by weakly cemented sand, and the dynamic soil properties of the Pacific Palisades site were assumed to be similar to those of the other two in order to investigate a slope of intermediate geometry. Detailed descriptions of the Seacliff and Daly City sites are presented below.

Seacliff State Beach

The Seacliff State Beach site (Fig. 7) is located just south of Santa Cruz, California. The coastal bluffs at the site are nearly vertical and about 30 m high. The terrain behind the crest of the slopes is flat and level for several hundred meters. The Seacliff site was selected due to its relatively simple geology and its record of



Fig. 7. Bluffs at Seacliff State Beach

observed failures during seismic events. Plant and Griggs (1990) provide a detailed description of slope failures at this site following the 1989 Loma Prieta earthquake and indicate that two types of failures occurred. Translation failures originating along joints or weathering surfaces occurred in the top 12 m of the bluffs. These failures were vertical in the Quaternary sediments and tended to flatten out in the Purisima formation. Tension cracks were observed extending 1–6 m behind the slope crests. The other type of failure was block sliding and toppling observed to occur over undercut bases. Failures of coastal bluffs were also observed in this general area during the 1906 San Francisco earthquake (Lawson 1908).

The results of the borehole logging and shear wave velocity testing (Fig. 8) at the Seacliff site were generally in agreement with the observations by Plant and Griggs (1990). The samples recovered from the boring indicated a surficial layer of sandy silt to a depth of 3.1 m, with an increasing sand content with depth. This material is the Quaternary period sand referred to by Plant and Griggs (1990). It is underlain by a poorly graded, uniform, fine sand to the terminal depth of the boring at 33 m. Based on

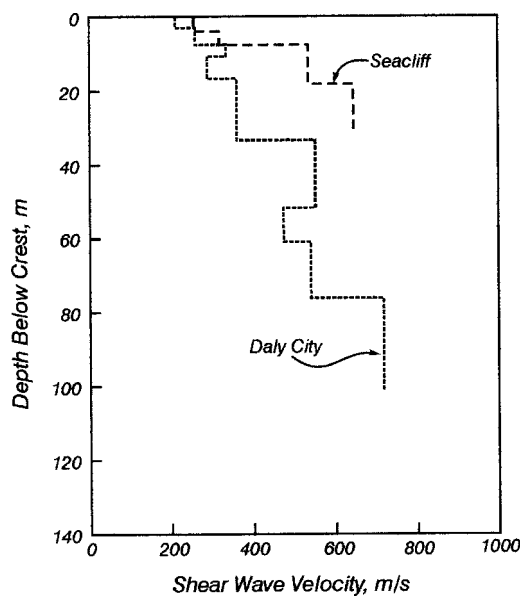


Fig. 8. Measured shear wave velocity profiles at Seacliff and Daly City sites

borehole samples, cementation within this stratum increases with depth, and the unit is a part of the Purisima formation.

Daly City

The Daly City site is located in the Westlake area of Daly City, California. Here, the coastal bluffs are moderately steep, with slopes between 40 to 55°, and attain heights in excess of 150 m. The bluffs face to the west. The terrain behind the crest of the bluffs is relatively flat, sloping approximately 5 degrees to the north.

Though the geology of this site is more complex than the Seacliff site, it was selected for analysis because of its geometry and because of its long history of failures during seismic events. Failures were documented along these bluffs in the 1906 and 1957 San Francisco earthquakes by Youd and Hoose (1978), and in the 1989 Loma Prieta earthquake as shown in Fig. 2 by Sitar (1991).

The field exploration at the Daly City site confirms the complex geology, and generally agrees with the description by Bonilla (1959). Samples from the boring indicate that the site is underlain by alternating layers of weakly cemented and uncemented, poorly graded sand and claystone of the Merced Formation to the terminal depth of the boring of 100 m. Sand layers dominate the profile and are typically uniformly graded, with layer thicknesses ranging from 3 to over 15 m. The clay is very stiff to hard, often slickensided, and occurs in layers up to 20 m thick. The measured shear wave velocity profile for the Daly City site is presented in Fig. 8.

Slope Models

Each model consists of a left and a right GCTB (Fig. 5), with each boundary divided into layers that are at most 0.1 wavelengths thick. This dimension is based on the strain-compatible shear wave velocity within the layer and the highest frequency of motion under consideration. The frequencies considered in the analyses were between 0.1 and 10 Hz, which is in the general range of engineering interest and contains the dominant frequencies of the seismograms used in the analyses.

Both the Seacliff and Daly City models were based on the results of the field exploration. The Seacliff model is a 27-m high, 75° slope that is representative of the specific conditions occurring at Seacliff State Beach. In order to determine the effect of the top boundary of the viscoelastic half-space, three different depths of this boundary were analyzed: 27, 41, and 67 m below the crest of the slope. The GCTB model for the Daly City site consists of a 116-m high, 45° slope with the viscoelastic half-space boundary located 134 m beneath the crest of the slope.

The Pacific Palisades model is based on the geometry of those slopes that failed during the 1994 Northridge earthquake, and consists of a 61-m high, 60° slope with a viscoelastic half-space boundary located 91 m below the crest of the slope. Since there is no site-specific data available for this site, the soil properties used in the analyses are based on the properties determined at the two other sites, which are typical for cemented sands. Though site specific properties would have been desirable, these analyses allow for a reasonable comparison of the response of a slope with geometry intermediate between the two other sites.

The strain-compatible shear wave velocity profiles used in the analysis for each site are presented in Fig. 9, and are significantly less than the low-strain values obtained from the downhole testing as presented in Fig. 8. The strain compatible soil properties were obtained from one-dimensional equivalent-linear site response analyses using the computer program SHAKE91 (Idriss and Sun

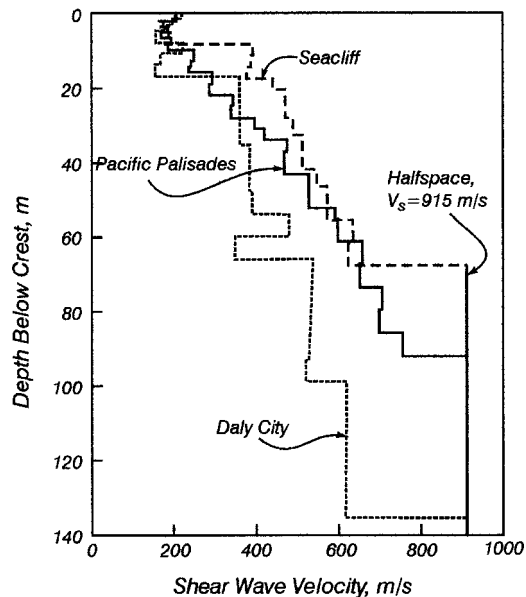


Fig. 9. Strain-compatible shear wave velocity profiles used in analysis of each site model

1992) with the UCSC0 record as the input rock outcrop motion. Relationships presented by Wang (1986) for the variation of normalized shear modulus and fraction of critical damping were used in the analyses. The strain-compatible soil properties obtained using the other two seismograms were very similar to those obtained from the UCSC0 record, and, in order to make a direct comparison between the different frequency contents of the earthquakes, the same strain-compatible profile was used in each analysis. The strain-compatible damping values in all models ranged from about 3 to 6%. Damping in the half-space was assumed to be 0.5%.

Seismograms Used in Analysis

The El Centro N/S seismogram from the May 18, 1940 El Centro earthquake ($M_w = 6.9$) was selected primarily because of its his-

torical use in slope and embankment response studies (e.g., Seed and Martin 1966). The peak acceleration in the record is 0.32 g and the dominant frequencies are between 5 and 6 Hz.

The UCSC0 seismogram was recorded at the University of California at Santa Cruz campus during the October 17, 1989, Loma Prieta earthquake ($M_s = 7.1$). The peak recorded acceleration at this station was 0.42 g. The dominant frequencies for this outcrop motion occur at 3 Hz and between 5 and 7 Hz. This record was selected because it likely has a frequency content representative of the motion experienced by the Seacliff site.

The JOS90 record is from the June 28, 1992, Landers earthquake ($M_s = 7.5$). This record was selected primarily because it contained low-frequency motion that was not observed in the other two records. The seismogram was recorded at the Joshua Tree Fire Station approximately 14 km from the epicenter. It has a peak acceleration of 0.28 g, and dominant frequencies near 1 and between 3 and 4 Hz.

Results

In each analysis, acceleration time histories were computed at the crest of the slope, in the free field behind the crest, and in front of the toe. The free-field response is taken as the one-dimensional response of the GCTB under consideration. The amplification of the motion at the crest of the slope was determined from the peak ground acceleration using the computed acceleration time histories.

Slope Crest Amplification

The comparison of the maximum acceleration computed at the crest of the slope and in the free field is presented in Table 1. The table shows the following information for each model: slope height (H), slope angle (S_1), Z/H ratio, and natural frequency of the soil profile behind the crest of the slope (f_n). The position of the half-space boundary relative to the slope crest is represented by the ratio Z/H , where Z is the depth to the half-space boundary below the slope crest, and H is the height of the slope (see Fig. 5). The site response is characterized by maximum acceleration at various locations (shown in Fig. 5) as follows: a_{fit} = maximum

Table 1. Summary of Results for Two-Dimensional Site Response Analyses

Site model	f_t (Hz)	Z/H	f_n (Hz)	Input motion	f_{eq} (Hz)	a_{fit} (g)	a_{fic} (g)	a_{max} (g)	A_t (%)	A_s (%)	A_a (%)
Seacliff $S = 75^\circ$, $H = 27$ m	2.46	2.44	1.76	ECNS	5-6	0.51	0.78	1.13	45	53	122
				UCSC0	3, 5-7	0.64	0.86	1.33	55	34	108
				JOS90	1, 3-4	0.30	0.45	0.65	44	50	117
		1.5	2.39	ECNS	5-6	0.48	0.84	1.21	44	75	152
				UCSC0	3, 5-7	0.66	1.04	1.55	49	58	135
				JOS90	1, 3-4	0.29	0.45	0.65	44	55	124
1.0	3.07	ECNS	5-6	0.32	0.81	1.15	42	153	259		
		UCSC0	3, 5-7	0.42	1.12	1.57	40	167	274		
		JOS90	1, 3-4	0.27	0.51	0.75	47	89	178		
Daly City $S = 45^\circ$, $H = 116$ m	0.75	1.16	0.85	ECNS	5-6	0.44	0.60	0.87	45	36	98
				UCSC0	3, 5-7	0.57	0.72	1.02	41	26	79
				JOS90	1, 3-4	0.28	0.48	0.75	56	71	168
Pacific Palisades $S = 60^\circ$, $H = 61$ m	1.26	1.5	1.32	ECNS	5-6	0.43	0.74	1.24	67	72	188
				UCSC0	3, 5-7	0.57	0.83	1.46	76	46	156
				JOS90	1, 3-4	0.27	0.52	0.79	52	92	192

free-field acceleration in front of the toe; a_{ffc} = maximum free-field acceleration behind the crest; and a_{max} = maximum crest acceleration. In addition, three measures of amplification are computed, “topographic amplification,” i.e., the amplification of the free-field motion at the crest; “soil amplification,” i.e., the amplification due to the differences in the soil columns in front of the toe and behind the crest, and “apparent amplification,” i.e., the apparent amplification of the motion between the base and the crest (Ashford and Sitar 1997).

Mathematically, these parameters are obtained as follows:

Topographic amplification:

$$A_t = \frac{a_{max} - a_{ffc}}{a_{ffc}} \quad (3)$$

Soil amplification:

$$A_s = \frac{a_{ffc} - a_{fft}}{a_{fft}} \quad (4)$$

Apparent amplification:

$$A_a = \frac{a_{max} - a_{fft}}{a_{fft}} \quad (5)$$

Consequently,

$$A_a = (1 + A_t)(1 + A_s) - 1 \quad (6)$$

Thus, the apparent amplification is completely described by the soil amplification and the topographic amplification. The apparent amplification is the parameter commonly noted in field studies of topographic effects following earthquakes, and it does not separate out the amplification due to the differences in the soil column between the crest and toe of the slope. In this paper, the topographic and soil amplification are treated separately in an attempt to determine the contribution of the different factors.

Overall, the results in Table 1 show that the average topographic amplification is on the order of 50%, compared with the average site amplification of over 70% and an average apparent amplification of over 150%. Perhaps more interesting is the range of values for the different measures of amplification: 40 to 76% for topographic amplification, as compared to between 26 to 167% for soil amplification. In general, the soil amplification has a much greater effect on the apparent amplification than does the topographic amplification, and the topographic amplification has much less variability than the soil amplification for the models studied.

A comparison of the data for each site shows that the greatest apparent amplification always occurs along with the greatest soil amplification. The converse is also true: the least apparent amplification occurs along with the least soil amplification. This further shows the primary dependence of the acceleration at the crest of the slope on the soil column rather than the topography.

The Seacliff models were also used to analyze the influence of the boundary of the half-space below the crest of the slope. The results show that A_s increases dramatically, from an average of 46% to an average of 136%, as Z/H decreases, the soil column gets shorter and the natural frequency of the deposit matches more closely the dominant frequencies of the input motion. In contrast, there is very little variance and no clear trend between A_t and Z/H , indicating that the topographic amplification is somewhat independent of the depth of the soil column. This is especially clear when contrasted to the strong dependence of soil amplification on the soil column.

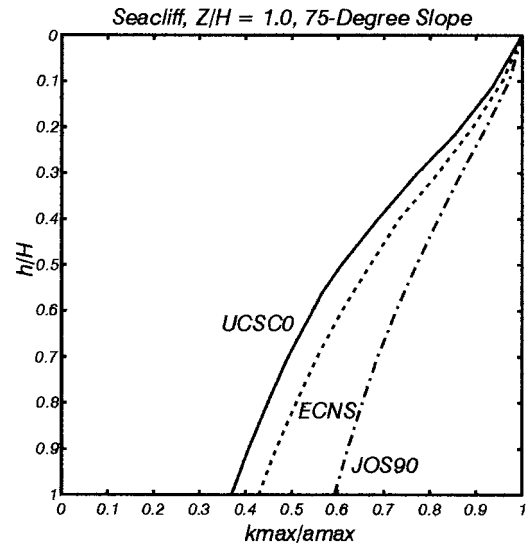


Fig. 10. Normalized maximum seismic coefficient profile for Seacliff model

In general, the results of the analyses of acceleration distribution in the models show that amplification due to the soil column is more important than topographic amplification. The effect of soil amplification is readily estimated using existing methods and it does vary predictably with the frequency content of the earthquake. Topographic amplification also varies with the frequency content of the earthquake; however, a simple relationship between frequency content and response is not evident from our paper. In general, topographic amplification, A_t , appears to be affected by a broadband of frequencies. However, the magnitude of A_t has a rather small range of values in the cases considered here, and in general, is on the order of 50%.

Maximum Average Seismic Coefficients

Time histories of average seismic coefficient, k_{av} , were developed as described above from the three input seismograms for each of the five site models as a function of the depth of the toe of the failure wedge (h). From each time history, the maximum average seismic coefficient, k_{max} , was selected, and a k_{max} profile for each model was developed. Similar to the procedure used in Makdisi and Seed (1978), the k_{max} profiles were normalized by the maximum crest acceleration of the model a_{max} . Profiles of k_{max}/a_{max} versus normalized depth, h/H , are presented in Fig. 10–12 for the Seacliff, Daly City, and Pacific Palisades models, respectively. For the Seacliff site, very little difference was found between each of the 3 models with varying depth of soil column, therefore, only the results for $Z/H = 1.0$ are shown. All results are summarized in Fig. 13 and compared to the range of values from Makdisi and Seed (1978).

An overall review of the results reveals a wider range of values than presented by Makdisi and Seed (1978), exceeding both the upper and lower bounds. The upper bound of this data is the Seacliff Model with the JOS90 motion, while the lower bound is the Daly City Model with the UCSC0 motion. For each site model, the shape of the profiles are similar, with the upper bound created by the JOS90 input motion in each case. The results from the UCSC0 and ECNS input motions are very similar within each set, the lower bound being formed by one or the other, or a combination of the two, depending on the model set.

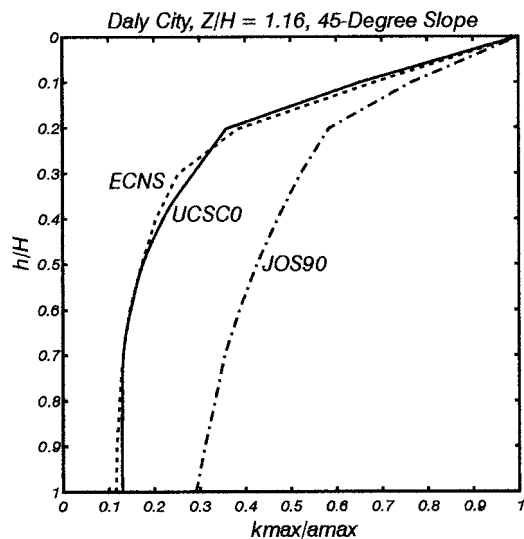


Fig. 11. Normalized maximum seismic coefficient profile for Daly City model

A comparison between profiles of k_{\max}/a_{\max} for different sites but the same input motion shows that the k_{\max}/a_{\max} profile tends to increase (i.e., shift to the right) with increasing slope angle. This is consistent for all input motions. As noted above, the k_{\max}/a_{\max} profiles for the Seacliff models using the same input motion, but varying H/Z (not shown) are very similar, indicating that the k_{\max}/a_{\max} profile is somewhat independent of the depth to the half-space boundary.

These results also indicate that the k_{\max}/a_{\max} profile is dependent on the frequency content of the earthquake, as exhibited by the comparison within sets; and the slope angle, as exhibited by the comparison between sets. The contrast between the profile shapes for the 75 and 45° slopes can be explained by focusing of the motion at the crest of the slope, and attenuation of the motion along the face of the flatter slope. This effect would result in the reduction of k_{\max}/a_{\max} as the failure surface extends down the

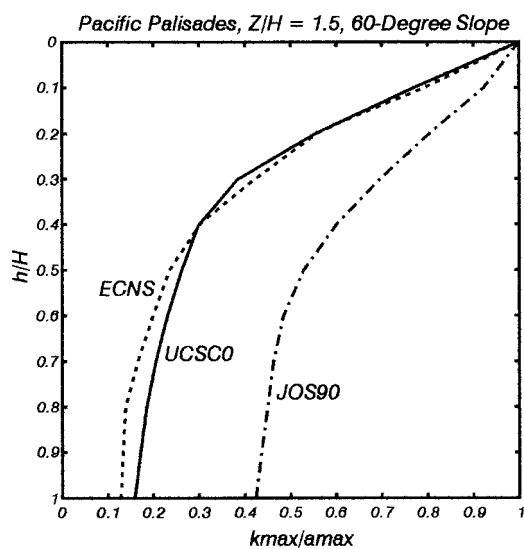


Fig. 12. Normalized maximum seismic coefficient profile for Pacific Palisades model

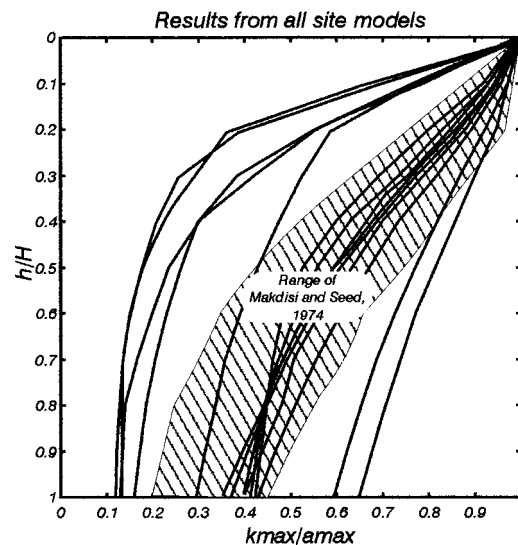


Fig. 13. Comparison of all maximum seismic coefficient profiles from this study with range of values from Makdisi and Seed (1978)

slope. In addition, points along the flatter slopes may be more out of phase with the crest motion than points along steeper slopes.

Proposed Procedure for Seismic Stability Analysis of Steep Slopes

Though the study presented herein was carried out specifically for steep slopes in weakly cemented sands, the procedures used in the seismic response portion of the study are equally applicable to steep slopes in other materials. Therefore, based on the above relationships between the peak acceleration at the crest and maximum seismic coefficient, a procedure for incorporating the results of this study into the stability analysis of steep slopes can be suggested, as follows:

1. The initial step should be a one-dimensional seismic site response analysis in the free field behind the crest of the slope using a suite of input motions appropriate for the site under consideration. When considering topographic effects, ample conservatism can be obtained by selecting an input motion with a dominant frequency close to the natural frequency of the site.
2. To account for the effect of topography, the maximum ground surface acceleration obtained by the one-dimensional analysis should be increased by 50% to estimate the maximum acceleration at the crest of the slope.
3. Normalized values of k_{\max} at various depths can be selected from the relationships presented in this paper. Upper bound values should be used for steepest slopes, while average values should be used for shallower slopes. The values of k_{\max} should be multiplied by 0.65, as suggested by Seed and Martin (1966), to obtain the k_{av} value to use for analysis.
4. This value of k_{av} can be used in traditional pseudostatic slope stability analyses, though it is recommended that other conditions specific to these steep slopes, including steep shallow failure planes and low tensile strengths, also be incorporated into the analyses.

Example Analysis

A brief example using the Seacliff State Beach site is given here in order to illustrate the use of the proposed procedure. Plant and

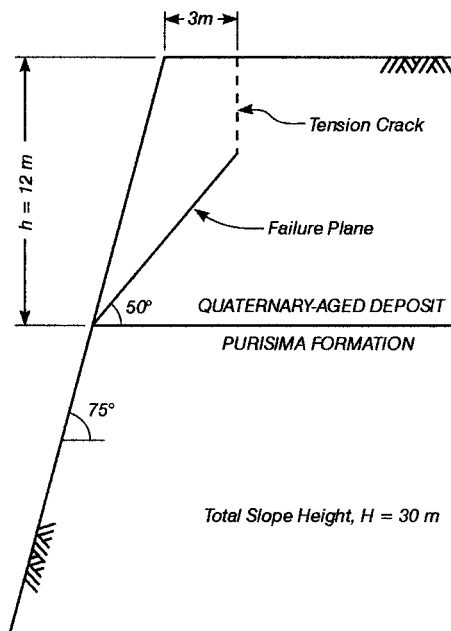


Fig. 14. Slope geometry used in example problem

Griggs (1990) provide a detailed description of slope failures at this site following the 1989 Loma Prieta earthquake and indicate translation failures originating along joints or weathering surfaces occurred in the top 12 m of the bluffs. The height (H) of the 75° slope is 27 m. Based on Plant and Griggs' (1990) observations, the base of most failure surfaces (h) was located 12 m below the crest of the slope, with tension cracks found up to 6 m behind the crest. Sitar et al. (1983) carried out an extensive laboratory investigation on quite similar materials in nearby Pacifica, California, and found that values of $c = 40$ kPa, $\phi = 38^\circ$, and a unit weight of 16.7 kN/m³ were typical of these types of materials. The proposed steps in determining the average seismic coefficient (k_{av}) are illustrated below. Once k_{av} is determined, an example pseudostatic analysis is carried out using the above materials properties.

To account for site effects, a one-dimensional equivalent linear site response analysis would normally be carried out at this stage. However, nearby strong motion records obtained from the Loma Prieta earthquake also provide the opportunity to show the effectiveness of the proposed procedure. In this example, the nearby CDMG Capitola Fire Station record will be used as representative of the free-field motion behind the crest. The mean peak horizontal ground acceleration from this record is 0.50 g (Campbell 1990). This assumed free-field motion is then multiplied by 1.5 to account for topographic amplification, resulting in a peak ground acceleration at the crest, a_{max} , of 0.75 g. The average seismic coefficient from Fig. 13 using the ratio of the depth to the base of the failure surface to the slope height ($h/H = 0.44$) results in a k_{max}/a_{max} value of 0.84. Therefore, k_{max} is 0.63 g. As suggested by Seed and Martin (1966), this value is multiplied by 0.65 to obtain the average seismic coefficient (k_{av}) of 0.41 g.

The stability analysis was carried out using the method proposed by Hoek and Bray (1981) for planar sliding surfaces, with tension cracks assumed to be located 3 and 6 m behind the crest, and failure planes assumed to be located between 40 and 50° from horizontal. The most critical case analyzed is shown in Fig. 14, with a static factor of safety of 1.59. Using the computed value of $k_{av} = 0.41$ g, we obtain a factor of safety to 0.95, which is consistent with the large number of failures observed in the area. For

this example slope, free-field accelerations as low of 0.43 g would be sufficient to lower the factor of safety to 1.00, which corresponds to an average seismic coefficient of 0.36. However, the value of $k_{av} = 0.36$ is still much higher than values typically used (e.g., Leshchinsky and San 1994) in pseudostatic slope stability analyses, and indicates that these slopes would likely be considered safe using currently accepted practice.

Conclusions

This paper has shown that because of the brittle nature of weakly cemented granular soils, a factor-of-safety-based approach, rather than a deformation-based approach, is most appropriate for these materials when considering seismic slope stability. Furthermore, based on site-response analyses using the generalized consistent transmitting boundary method, it was concluded that soil effects dominate the seismic response of steep slopes. More specifically, the effect of the soil column behind the crest of a steep slope, though quite variable, can have a much greater affect on the seismic response than the effect of topography. In this paper, topographic amplification was defined as the amplification at the slope crest as compared to the free-field motion *behind the crest*, rather than comparing the crest motion to the base motion. Using this definition, the effect of the soil column could be factored out. It was found that the amount of amplification due to topography is relatively consistent between different slope geometries and soil profiles, and is on the order of 50%.

Based on the field and laboratory observations presented in this paper, together with analyses carried out herein, a new simplified method to assess the seismic stability of steep slopes is presented. This pseudostatic method uses average seismic coefficients to account for the effect of topographic amplification. This method can be used along with traditional slope stability analysis procedures as long as factors specific to these steep slopes are properly accounted for (e.g., shallow planar failure surfaces and tension cracks). Though this method was developed for slopes in California, and specifically validated for slopes that failed in the Loma Prieta earthquake, it should be applicable to steep slopes elsewhere along the Pacific Coast, and to steep slopes in general.

Acknowledgments

This research was supported by the U.S. Geological Survey under USGS Award No. 14-08-0001-G2127. The views and conclusions contained in this paper are those of the writers and should not be interpreted as necessarily representing the official policies, either expressed or implied, of the U.S. Government. The financial support of the donors is greatly appreciated by the writers.

Notation

The following symbols are used in this paper:

- A_t = topographic amplification;
- A_s = soil amplification;
- A_a = apparent amplification;
- a_{ffc} = maximum free-field acceleration behind the crest;
- a_{fft} = maximum free-field acceleration in front of toe;
- a_{max} = maximum crest acceleration;
- c = cohesion intercept;

f_n = natural frequency of soil profile behind crest of slope;
 H = height of slope;
 h = depth to base of failure surface;
 k_{av} = average maximum seismic coefficient;
 k_{max} = maximum seismic coefficient;
 M = mass of failure wedge;
 $m(y)$ = mass of slice at depth y ;
 S_1 = slope angle;
 S_2 = angle of failure plane;
 $\ddot{u}_a(y)$ = absolute acceleration of slice;
 $x_1, x_2,$ = vertical dimensions;
 Z = depth to half-space surface;
 ΔM = slice weighting; and
 ϕ = angle of internal friction.

References

- Acar, Y. B., and El-Tahir, E. A. (1986). "Low strain dynamic properties of artificially cemented sand." *J. Geotech. Eng.*, 112(11), 1001–1015.
- Airey, D. W. (1993). "Triaxial testing of naturally cemented carbonate soil." *J. Geotech. Eng.*, 119(9), 1379–1398.
- Ashford, S. A., and Sitar, N. (1994). "Seismic response of steep natural slopes." *Rep. No. UCB/EERC 94-05*, Earthquake Engineering Research Center, College of Engineering, Univ. of California at Berkeley, Berkeley, Calif.
- Ashford, S. A., and Sitar, N. (1997). "Analysis of topographic amplification of inclined shear waves in a steep coastal bluff." *Bull. Seismol. Soc. Am.*, 87(3), 692–700.
- Ashford, S. A., Sitar, N., Lysmer, J., and Deng, N. (1997). "Topographic effects on the seismic response of steep slopes." *Bull. Seismol. Soc. Am.*, 87(3), 701–709.
- Baig, S., Picornell, M., and Nazarian, S. (1997). "Low strain shear moduli of cemented sands." *J. Geotech. Geoenviron. Eng.*, 123(6), 540–545.
- Bonilla, M. G. (1959). "Geologic observation in the epicentral area of the San Francisco earthquake of March 22, 1957." *Special Rep. 57*, G. B. Oakenshott, ed., California Division of Mines, 25–37.
- California Division of Mines and Geology. (1997). "Guidelines for evaluating and mitigating seismic hazards in California." *Special Publication 117*, Department of Conservation, Sacramento, Calif.
- Campbell, K. W. (1990). "An empirical analysis of peak horizontal acceleration for the Loma Prieta, California earthquake of 18 October 1989." *Bull. Seismol. Soc. Am.*, 81(5), 1838–1858.
- Clough, G. W., Sitar, N., Bachus, R. C., and Rad, N. S. (1981). "Cemented sands under static loads." *J. Geotech. Eng.*, 107(6), 799–817.
- Das, B. M., Yen, S. C., and Dass, R. N. (1995). "Brazilian tensile strength test of lightly cemented sand." *Can. Geotech. J.*, 32, 166–171.
- Deng, N. (1991). "Two-dimensional site response analyses." Thesis, Univ. of California at Berkeley, Berkeley, Calif., in partial satisfaction of the requirements for the degree of Doctor of Philosophy.
- Haruyama, M. (1973). "Geological, physical, and mechanical properties of Shirasu and its engineering classification." *Soils Found.*, 13(3), 45–60.
- Huang, J. T., and Airey, D. W. (1998). "Properties of artificially cemented carbonate sand." *J. Geotech. Geoenviron. Eng.*, 124(6), 492–499.
- Hynes, M. E., and Franklin, A. G. (1984). "Rationalizing the seismic coefficient method." *Miscellaneous Paper GL-84-13*, U.S. Army Corps of Engineers, Waterways Experiment Station, Vicksburg, Miss.
- Idriss, I. M., and Seed, H. B. (1967). "Response of earthbanks during earthquakes." *J. Soil Mech. Found. Div., Am. Soc. Civ. Eng.*, 93(SM3), 61–82.
- Idriss, I. M., and Sun, J. I. (1992). *User's Manual for SHAKE91*, Center for Geotechnical Modeling, Dept. of Civil and Environmental Engineering, Univ. of California, Davis, Calif.
- Kovacs, W. D., Seed, H. B., and Idriss, I. M. (1971). "Studies of seismic response of clay banks." *J. Soil Mech. Found. Div., Am. Soc. Civ. Eng.*, 97(SM2), 441–455.
- Kramer, S., and Smith, D. (1997). "Modified newmark model for seismic displacements of compliant slopes." *J. Geotech. Geoenviron. Eng.*, 123(7), 635–644.
- Lawson, A. C. (1908). "California Earthquake of April 18, 1906." *Publication No. 87*, Report to the State Earthquake Investigation Committee, Vol. 1. Carnegie Institute of Washington, Washington, D.C.
- Leshchinsky, D., and San, K.-C. (1994). "Pseudostatic seismic stability of slopes: Design charts." *J. Geotech. Eng.*, 120(9), 1514–1532.
- Lysmer, J., and Waas, G. (1972). "Shear waves in plane infinite structures." *J. Eng. Mech. Div., Am. Soc. Civ. Eng.*, 98(EM1), 85–105.
- Makdisi, F. I., and Seed, H. B. (1977). "A simplified procedure of estimating earthquake-induced deformations in dams and embankments." *EERC Research Report, No. UCB/EERC-77/19*.
- Makdisi, F. I., and Seed, H. B. (1978). "Simplified procedure for estimating dam and embankment earthquake-induced deformations." *J. Geotech. Eng. Div., Am. Soc. Civ. Eng.*, 104(GT7), 849–867.
- Mononobe, N., Takata, A., and Matumura, M. (1936). "Seismic stability of the earth dam." Section and Congress on Large Dams, Washington, 4(1936), 435–442.
- Newmark, N. M. (1963). "Effects of earthquakes on dams and embankment." *Paper presented at the ASCE Structural Engineering Conf.*, San Francisco.
- Newmark, N. M. (1965). "Effects of earthquakes on dams and embankment." *Geotechnique*, 15(2), 131–160.
- O'Rourke, T. D., and Crespo, E. (1988). "Geotechnical properties of cemented volcanic soil." *J. Geotech. Eng.*, 114(10), 1126–1147.
- Plant, N., and Griggs, G. B. (1990). "Coastal landslides caused by the October 17, 1989 earthquake." *Calif. Geol.*, 43(4), 75–84.
- Puppala, A. J., Acar, Y. B., Tumay, M. T. (1995). "Cone penetration in very weakly cemented sand." *J. Geotech. Eng.*, 121(8), 589–600.
- Sarma, S. K. (1975). "Seismic stability of earth dams and embankments." *Geotechnique*, 25(4), 743–761.
- Seed, H. B., and Goodman, R. E. (1964). "Earthquake stability of slopes of cohesionless soils." *J. Soil Mech. Found. Div., Am. Soc. Civ. Eng.*, 90(SM6), 43–73.
- Seed, H. B., and Martin, G. R., (1966). "The seismic coefficient in earth dam design." *J. Soil Mech. Found. Div.*, 92(SM3), 25–58.
- Sitar, N. (1990). "Seismic response of steep slopes in weakly cemented sands and gravels." *Proc., H. Bolton Seed Memorial Symposium*, Vol. II, BiTech, Ltd., Vancouver, BC, Canada, 67–82.
- Sitar, N. (1991). "Earthquake-induced landslides in coastal bluffs and marine terrace deposits." *Special Publication No. 1, Loma Prieta Earthquake*, Association of Engineering Geology, 75–82.
- Sitar, N., and Clough, G. W. (1983). "Seismic response of steep slopes in cemented soils." *J. Geotech. Eng., Am. Soc. Civ. Eng.*, 109(2), 210–227.
- Wang, Y. D. (1986). "Investigation of constitutive relations for weakly cemented sands." PhD dissertation, Dept. of Civil Engineering, Univ. of California, Berkeley, Calif., p. 293.
- Youd, T. L., and Hoose, S. H. (1978). "Historic ground failures in Northern California triggered by earthquakes." *Geological Survey Professional Paper 993*, U.S. Government Printing Office, Washington, D.C.